Optical phonons in $Pb_{1-x}Eu_xTe$ epilayers and PbTe/EuTe superlattices: Berreman effect

M. Aigle and H. Pascher
Experimentalphysik I, Universität Bayreuth, D-95440 Bayreuth, Germany

Hyunjung Kim,* E. Tarhan, A. J. Mayur,† M. Dean Sciacca,‡ and A. K. Ramdas
Department of Physics, Purdue University, West Lafayette, Indiana 47907

G. Springholz and G. Bauer
Institut für Halbleiterphysik, Universität Linz, A-4040 Linz, Austria
(Received 3 January 2001; published 25 June 2001)

The frequencies of the zone-center optical phonons in $Pb_{1-x}Eu_xTe$ ($0 \leqslant x \leqslant 1$) epilayers both grown by molecular beam epitaxy and of the confined optical phonons in PbTe/EuTe superlattices have been determined from the transmission minima in the far infrared. With radiation incident on the film normally, only the transverse optical (TO) phonons can be observed, whereas oblique incidence allows the appearance of the longitudinal optical (LO) phonons as well, due to the Berreman effect. The first-order infrared spectrum of $Pb_{1-x}Eu_xTe$ exhibits a pair of ''EuTe-like'' zone-center optical phonons originating in the localized mode of Eu in PbTe and evolving into the LO-TO pair of EuTe; the LO modes appear only in the oblique Berreman geometry, the radiation being polarized in the plane of incidence. From a high-quality EuTe epilayer, the frequencies of the TO and the LO phonons at 5 K have been determined to be 109.5 cm^{-1} and 147.2 cm^{-1}, respectively. The phonon dispersion for EuTe with finite wave vectors along $\langle 111 \rangle$ has been deduced from the *confined* TO and LO modes observed in $(PbTe)_m/(EuTe)_n$ superlattices.

DOI: 10.1103/PhysRevB.64.035316 PACS number(s): 78.30.Hv, 63.20.Dj, 63.22.+m

I. INTRODUCTION

Mn- and Eu-based IV-VI diluted magnetic semiconductors are attractive for basic investigations as well as for optical applications, due to the magnetism associated with their magnetic constituent (Mn^{2+} or Eu^{2+}) and the extensive tunability of their band gaps from the midinfrared to the visible region. Magneto-optical investigations have been reported in the entire composition range of $Pb_{1-x}Eu_xTe$ including EuTe.[1,2] Mid-infrared lasers based on $Pb_{1-x}Eu_xTe$ have expanded the number of lasers that utilize the band-gap engineering of the Pb chalcogenides.[3–6]

EuTe is an antiferromagnetic semiconductor with a Néel temperature of 9.7 K. Its magnetic properties and bandstructure have been the subject of several studies.[7–9] Its lattice vibrations have been investigated using magnetic-phase-induced Raman scattering,[10] infrared reflection,[11] and absorption[12] spectroscopy.

Modern nonequilibrium growth techniques such as molecular beam epitaxy (MBE) have made the fabrication of PbTe/EuTe superlattices possible. They have led to studies in which the magnetic interaction between the EuTe layers through the diamagnetic PbTe barriers have been addressed. Such studies are important for obtaining insights into the underlying magnetic exchange mechanisms.

In the context of a complete material characterization, the importance of lattice vibrational, in addition to electronic and magnetic properties, has been well recognized. Various effects involving electron-phonon interaction further underscore the significance of such investigations. Infrared reflection and transmission as well as Raman spectroscopy are typically exploited to discover and delineate important features of the phonon dispersion. $Pb_{1-x}Eu_xTe$, including the end members PbTe and EuTe, crystallize in the *NaCl structure*. As a consequence of the *rule of mutual exclusion in centro-symmetric crystals*, their zone-center transverse optical (TO) and longitudinal optical (LO) phonons are *infrared allowed but Raman forbidden.* In contrast to materials with the zinc-blende structure, the TO and LO phonons in materials with the NaCl structure are accessible only in infrared spectroscopy. It is possible to resort to defect- or spin-induced one-phonon Raman scattering, but its observation is experimentally demanding and interpretation less straightforward. In the range of low Eu concentration, and hence narrow energy gaps, Raman scattering using visible excitation is again not generally profitable in view of the small penetration depth.

As a consequence of the large electric dipole moment associated with the zone-center optical modes of polar crystals like the Pb salts, one can investigate their infrared activity in bulk specimens only in reflectivity. The reststrahlen spectrum thus obtained has to be subjected to a curve-fitting procedure in which ω_{TO}, the dielectric constants ϵ_0 and ϵ_∞, and the damping constant γ are the adjustable parameters or experimental inputs. Thus the frequencies of TO and LO modes are obtained with a computer-intensive procedure.

Barnes and Czerny[13] were the first to directly measure the TO-phonon frequency in thin alkali halide films using transmission spectroscopy at normal incidence. In contrast, the Berreman effect[14] allows a *direct* observation of *both* kinds of phonons in films that are small in thickness compared to the wavelength of the electromagnetic radiation corresponding to that of the reststrahlen band. With radiation at oblique incidence and with the electric vector polarized perpendicular to the plane of incidence, i.e., in *s* polarization, there is only one transmission minimum at ω_{TO}, but for the

electric vector polarized parallel to the plane of incidence, i.e., in *p* polarization, transmission minima are observed at both ω_{TO} and ω_{LO}. At normal incidence, only the minimum at ω_{TO} is observed, independent of polarization. Its application for the investigation of zinc-blende semiconductor epilayers and superlattices has been exploited by Sciacca *et al.*[15] Kliewer *et al.*[16] and Kliewer and Fuchs[17,18] have analyzed the transmission and reflectivity of an ionic crystal slab in terms of virtual modes involving radiative and nonradiative mixed excitations. Proix and Balkanski[19] have summarized this approach and presented a physical picture more accessible for comparison with experimental results. In particular, they show that, for thicknesses (d) satisfying $(\omega_{TO}d/c) \ll 1$, the minima observed in infrared transmission indeed correspond to the bulk ω_{TO} and ω_{LO} as deduced by Berreman.[14] The specimens employed in our measurements do indeed fulfill this criterion.

Far-infrared spectroscopy of superlattices has been studied in transmission[20] and reflectivity[21–23] spectroscopy.

In the present paper, we report the zone-center optical phonons in MBE-grown films of EuTe and $Pb_{1-x}Eu_xTe$ ($0 \leqslant x \leqslant 1$) and confined optical phonons in PbTe/EuTe superlattices using the Berreman technique. From the superlattice data, we determine the optical phonon dispersion of EuTe. Inelastic neutron scattering as a means of determining the phonon dispersion curve is not available for EuTe because of the large absorption cross section of Eu for slow neutrons.[24]

II. EXPERIMENT

A. Sample growth and preparation

$Pb_{1-x}Eu_xTe$ layers, 3 to 4.6 μm in thickness, were grown directly on (111) BaF_2 substrates in a RIBER 1000 MBE machine. They were characterized after deposition with high-resolution x-ray diffraction. As expected for the (111) substrate, the epilayers displayed a (111) orientation. The full width at half maximum of the (222) layer peak increased from $\sim$65 arcsec for $x=0.02$ to 260 arcsec for $x=0.92$. The sample with $x=0.81$ was the only one that did not occur in a single phase. The Eu content (x) has been obtained using atomic emission spectroscopy and is in good agreement with the values given by the flux calibration of MBE. From Hall measurements, the free-electron concentrations have been deduced to be in the range of 1.1×10^{17} cm^{-3} to 4.4×10^{17} cm^{-3} for small x, and for $x>0.2$, the specimens are semi-insulating. For the PbTe/EuTe superlattices, a 0.3 μm to 4 μm thick PbTe buffer layer was grown on the (111) BaF_2 substrate. The superlattice consists of 40 to 400 periods of $(PbTe)_n/(EuTe)_m$ with the number of PbTe monolayers, n, between 1 and 42 and those of EuTe, m, between 1 and 14 monolayers. For the details of the MBE growth and x-ray characterization see Refs. 25–29. In order to avoid channeling in the infrared transmission, a wedge was introduced in the BaF_2 substrates of all the samples.

B. Infrared transmission spectroscopy

The infrared transmission spectra were recorded with a BOMEM DA3 Fourier transform infrared spectrometer,[30] employing a mercury source and a Mylar beam splitter. No polarizer was employed in the experiments; the *p*-polarized LO phonon observed in oblique incidence thus appears superposed on the *s*-polarized, unabsorbed radiation. The transmission experiment was carried out with a resolution of 0.5 cm^{-1} and typical spectra were obtained with 50–100 co-additions. A composite Si bolometer,[31] operating at 4.2 K with a long-pass cold filter and cone optics, was used as a detector. The samples were cooled to 5 K in a Janis Supervaritemp 10DT optical cryostat[32] with polypropylene windows.

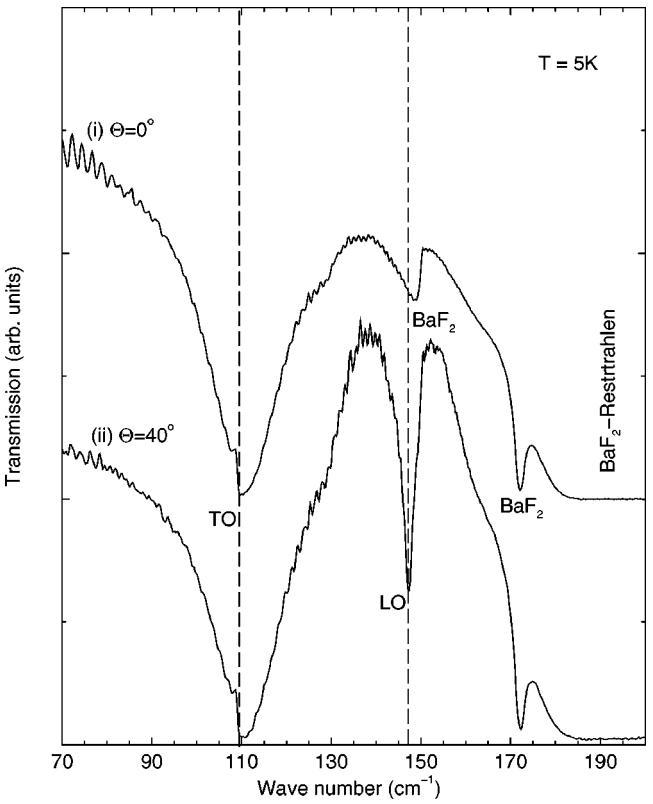

FIG. 1. Infrared transmission spectrum of an EuTe epilayer measured at 5 K: (i) normal incidence and (ii) oblique incidence. The sharp transmission minima corresponding to TO and LO phonons are identified in the figure with vertical lines.

III. RESULTS AND DISCUSSION

A. Zone-center optical phonons in EuTe

The infrared transmission spectrum of a 2 μm thick EuTe epilayer grown on a (111) BaF_2 substrate is displayed in Fig. 1 for (i) normal and (ii) oblique incidence. One can clearly see the minimum corresponding to the zone-center TO phonon in both geometries, whereas that corresponding to the zone-center LO phonon appears only in oblique incidence. The TO- and LO-phonon frequencies directly read from the positions marked by dashed lines are 109.5 and 147.2 cm^{-1}, respectively. The broad absorption above the LO frequency and the structures at 150 and 172 cm^{-1} are due to the BaF_2 substrate.[33]

TABLE I. The zone-center TO and LO frequencies of EuTe (in cm^{-1}) obtained from various methods.

Method	TO	LO	Temperature
ir reflectivity[a]	102.3±2	141.5±2	300 K
Raman[b]		145	1.8 K
ir absorption[c]	111.7		2 K
Berreman (present work)	109.5	147.2	5 K

[a]Reference 11.
[b]Reference 10.
[c]Reference 12.

In Table I we compare our values for the TO and LO frequencies with those cited in the literature. As can be seen, the agreement between the low-temperature values is excellent. Holah *et al.*[11] have deduced their values from a fit to the reflectivity spectrum using a single oscillator model. Schmutz *et al.*[10] observed the zone-center LO phonon in spin-dependent Raman scattering in a magnetic field. Ikezawa and Suzuki[12] reported the zone-center TO phonon in the absorption spectrum of evaporated EuTe films, but detected only the infrared-active TO phonon at the Γ point, presumably because they employed normal incidence in their measurements. The present study on MBE-grown samples has revealed both TO and LO phonons in the oblique geometry. The simplicity of the Berreman technique, the high signal to noise ratio in the spectra recorded, the sharpness of the spectral features at the lower temperature, and the high quality of the samples have contributed to the quality of the results reported here.

From the channeled spectrum in the optical transmission well below the band gap of EuTe at 2.27 eV, a refractive index (n) of EuTe of $n=2.16$ is obtained. From the optical dielectric constant $\epsilon_\infty = n^2 = 4.66$ and the Lyddane-Sachs-Teller relation, i.e. $(\omega_{LO}/\omega_{TO}) = (\epsilon_0/\epsilon_\infty)^{1/2}$, the static dielectric constant ϵ_0 is deduced as 8.42. Our values are consistent with those reported by Holah *et al.*[11]

B. Multimode behavior in $Pb_{1-x}Eu_xTe$ epilayers

Figure 2 shows the transmission spectra of $Pb_{1-x}Eu_xTe$ for a representative set of x. The frequencies of the minima, labeled as TO_1 and LO_1, are displayed as a function of x in Fig. 3. As $x \to 1$, they extrapolate to those of the TO and LO modes of pure EuTe; the single frequency to which the TO and LO values converge as $x \to 0$ is ascribed to the local mode of Eu in PbTe. Whereas the TO_1 mode can be observed in oblique and normal incidence, the LO_1 mode only appears in oblique incidence. Both modes decrease in intensity with decreasing x.

The ''PbTe-like'' modes are expected to evolve from the TO- and LO-phonon modes in PbTe at 17 cm^{-1} and 108 cm^{-1}, respectively.[34] The PbTe TO phonon is observed as a strong and broad absorption band whose range appears to extend below 20 cm^{-1} where reliable data have yet to be obtained. The PbTe LO phonon could be observed in pure PbTe at 109 cm^{-1}. As expected, it appears in oblique incidence only and is weak compared to the TO phonon. The LO

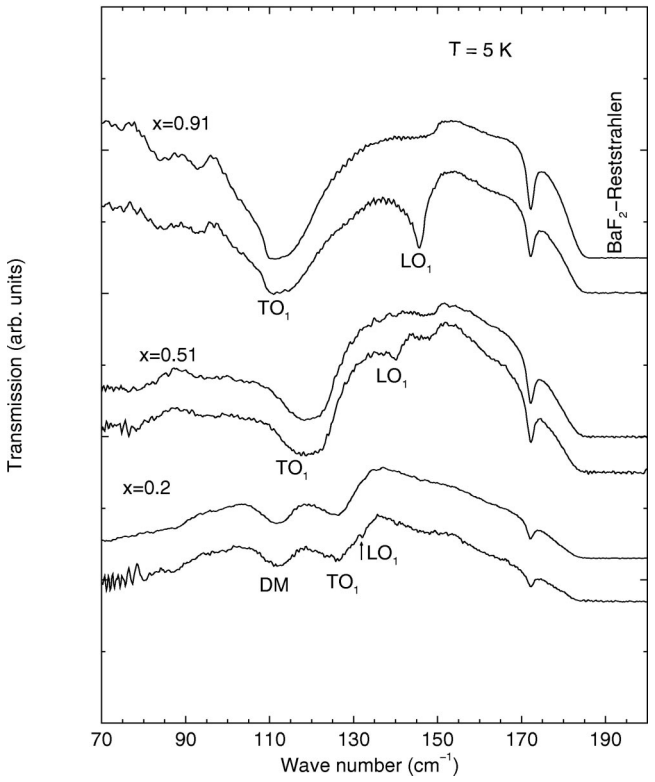

FIG. 2. Infrared transmission spectra of $Pb_{1-x}Eu_xTe$ epilayers at 5 K for selected values of x. In each pair of spectra shown, the upper spectrum was recorded at normal and the lower at oblique incidence.

mode for PbTe in the presence of $\sim 10^{17}$ cm^{-3} free electrons can be expected to have experienced a shift to ω_+, the higher-frequency plasmon-phonon coupled mode, at ~ 200 cm^{-1}, based on theory for such excitations.[35] Hence it is intriguing that the value observed in the present work coincides with the literature value of the pure LO phonon. A possible speculation is that the observed weak feature originates from an absorption in a surface depletion layer.

The x dependence of the frequencies of the zone-center optical phonons, i.e., the mode behavior of alloys is usually classified as ''one-mode,'' ''two-mode,'' and ''one-two-mode,'' behavior. Different approaches have been developed for predicting such mode behavior.[36] The simple consideration of the absence of an overlap in the reststrahlen bands of the end members of a ternary alloy favors a two mode behavior in $Pb_{1-x}Eu_xTe$. A criterion based on the relative masses, however, would predict a one-mode-behavior.[37] A more comprehensive mode criterion based on the Saxon-Hutner theorem, described in Ref. 38, can be formulated in which one takes into account the existence or absence of an overlap in the phonon dispersion of the end members. In our case, the frequencies of the PbTe LO phonon and of the EuTe TO phonon come very close, and a small overlap in the density of states cannot be excluded. Indeed, from calculations by Ousaka *et al.*[39] and neutron data by Cochran *et al.*,[40] an overlap exists. However, the convergence of the two ''EuTe-like'' phonon frequencies to that of a local mode as $x \to 0$ in $Pb_{1-x}Eu_xTe$ suggests a two- rather than one-mode behavior.

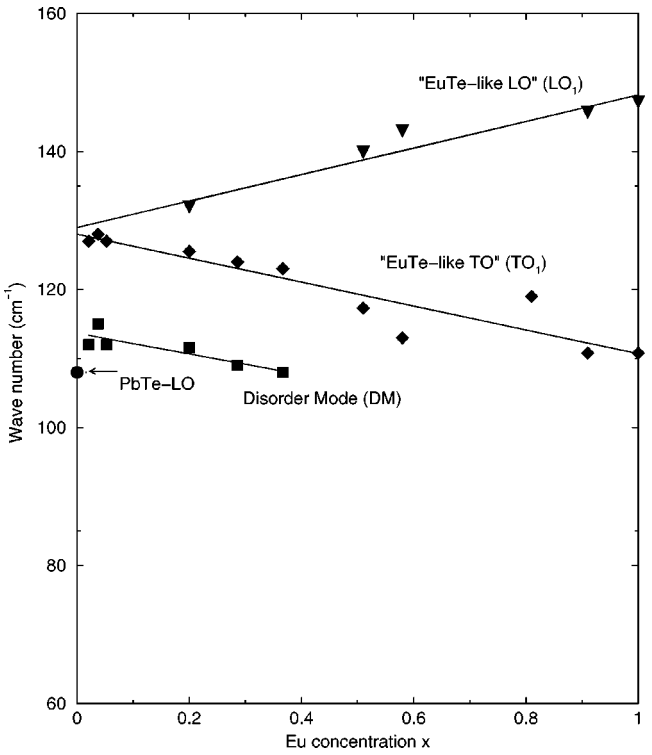

FIG. 3. The frequencies of the $Pb_{1-x}Eu_xTe$ zone-center optical phonons and of a disorder induced mode (DM) as a function of x. The solid lines are a guide to the eye. The weaker LO signatures for $x=0.29$, $x=0.37$, and $x=0.81$ are lost in the noise because of the specimen quality; for these samples, only ω_{TO} deduced from the stronger TO phonon is displayed.

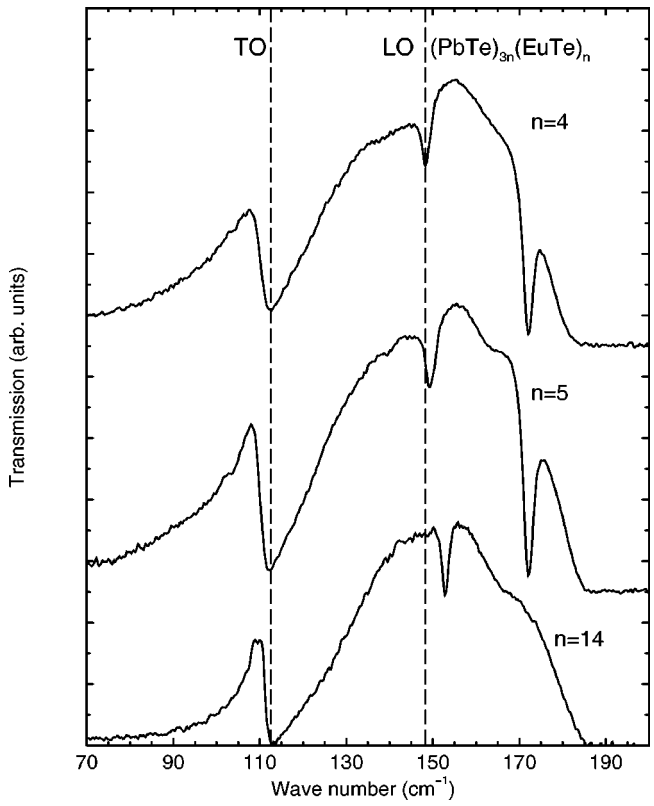

FIG. 4. Infrared transmission spectra of $(PbTe)_{3n}(EuTe)_n$ superlattices with $n=4$, 5, and 14. The dashed lines mark the position of the confined TO and LO phonons for $n=4$. All the spectra shown were obtained in oblique incidence. The feature at 172.5 cm^{-1} is due to an unknown impurity in the BaF_2 substrate, not present in all the samples.

For $x>0$, a mode labeled DM, for disorder mode, appears, which shows a maximum intensity at $x=0.05$; it becomes weaker and finally disappears for large x. Even though it is observed for small x with frequencies very close to the LO-phonon mode of PbTe, we do *not* ascribe it to the PbTe-like LO phonon for two reasons: (1) In contrast to the behavior of the 109 cm^{-1} minimum in PbTe that disappears at normal incidence, it shows no significant dependence on the angle of incidence of radiation. (2) It reaches a maximum strength around $x=0.05$, rather than at $x=0$ as one would expect for PbTe-like LO phonons. We propose that the observed DM mode is due to alloy disorder and the associated breakdown of translational symmetry. The frequency distribution of lattice vibrations of PbTe calculated by Cochran *et al.*[40] indeed shows a distinct peak around 100 cm^{-1}, not too different from that of the DM feature.

C. Confined optical phonons in $(PbTe)_m/(EuTe)_n$ superlattices: EuTe phonon dispersion

Superlattices offer a very attractive opportunity to deduce the dispersion curves of optical phonons of the constituent layers from infrared and Raman measurements.[41] If phonons with frequencies allowed in one of the constituents of the superlattice cannot propagate in the other, they are designated as *confined*. Requiring that their amplitudes vanish at the layer boundaries, phonons appear as standing waves in each constituent with discrete wave vectors $|\mathbf{q}_l|$ given by l/n in units of $\pi\sqrt{3}/a$. It is implicitly assumed that the standing waves are entirely confined without any leakage; this is in contrast to similar considerations in, for example, GaAs/AlAs (Ref. 41) and CdTe/ZnTe (Ref. 42). The good agreement between a linear chain model and the experimental data justifies this assumption. Here a is the lattice constant, n is the number of monolayers of the material considered, and the integer l specifies the order of the confined phonon. Only excitations with an odd l are infrared active, their intensity being proportional to l^{-2}.

We investigated confined phonons of EuTe in a series of (111) $(PbTe)_m/(EuTe)_n$ superlattices with EuTe monolayers having $n=1$ to 14. This has allowed us to determine the frequencies of phonons with q's along the Λ direction in the Brillouin zone. Figure 4 shows a selection of transmission spectra for different values of n with $m=3n$, obtained at oblique incidence. The position of the TO phonon does not show a significant change with n, but that of the LO phonon exhibits a distinct shift. At normal incidence, only TO is observed in all the samples. We have assumed that the TO phonons of EuTe are confined in spite of the overlap of the LO branch of PbTe with the TO branch of EuTe as indicated by the proximity of EuTe(TO) at 109.5 cm^{-1} and PbTe(LO) at 109 cm^{-1}. Our assumption is justified by the difference

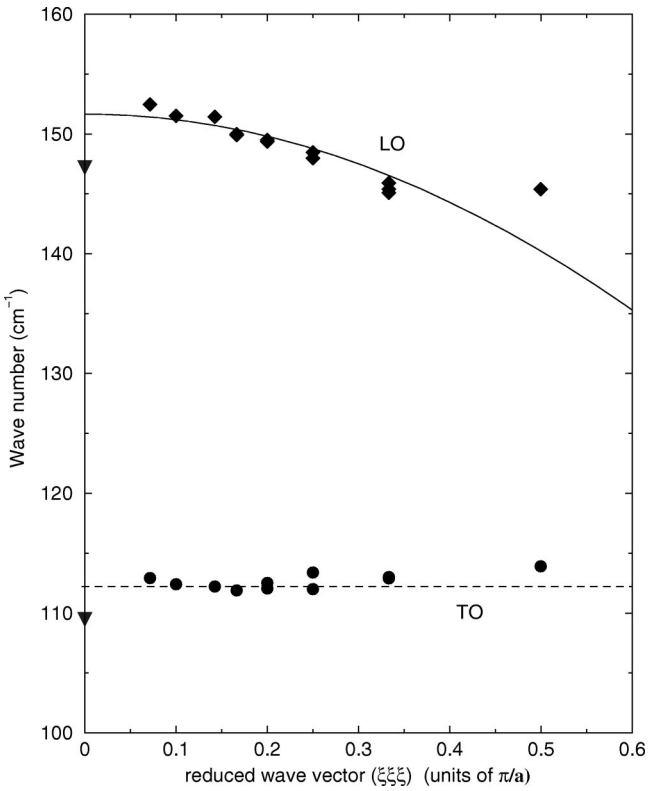

FIG. 5. The dispersion of the LO and TO phonons of EuTe deduced from the confined optical phonons in $(PbTe)_m(EuTe)_n$ along the Λ direction, i.e., along $\langle 111 \rangle$. The solid line for the LO phonons is computed from a linear chain model. The line for the TO phonons is a guide to the eye.

in the polarization of the corresponding eigenvectors of the modes. In samples with $n=1$ and $n=2$, no sharp minima could be seen at the TO and LO positions; in such extremely thin layers, monolayer fluctuations could very well obliterate the phonon signature. Figure 5 shows the plot of the confined phonon frequencies versus wave vector in the Λ direction. The solid line shows the result of a simple linear chain model calculation for LO modes, using the force constant as a fitting parameter. The data points at $q=0$ are taken from the spectra of the 2 μm EuTe layer; they are lower in frequency than the value obtained from the extrapolation of the data from superlattices. This discrepancy appears to be related to the strain produced by the lattice mismatch between EuTe and PbTe.[27] In contrast, the 2 μm thick EuTe epilayer, grown directly on the BaF_2 substrate, can be assumed to be completely relaxed. In this context, our LO and TO phonon dispersion relation are characteristic of strained layers. In the absence of the values for the deformation potential constants for the LO and TO phonons of EuTe, a quantitative correction for strain has to be deferred. It has also been pointed out in the literature[23] on the AlAs/GaAs superlattices that interface roughness and disorder effects may have influence on the phonon frequencies and hence on the dispersion curves. A quantitative correction of the phonon frequencies would require detailed knowledge about such imperfections. Also, x-ray diffraction measurements have shown that MBE allows the growth of PbTe/EuTe superlattices with excellent structural properties and smooth heterointerfaces.[26] These considerations can be addressed with a more comprehensive characterization of the nature and concentration of defects, on the one hand, and model calculations on the other.

IV. CONCLUDING REMARKS

The present study shows how the Berreman technique can be profitably applied to investigate phonons in alloys and superlattices of NaCl structure, where the phonons are Raman forbidden; besides, the longitudinal and transverse character of the phonons emerge naturally in the Berreman effect for a high-symmetry direction, $\langle 111 \rangle$ in our case. Applying this technique to a EuTe epilayer, we determine accurate low-temperature values for the zone-center TO (109.5cm^{-1}) *and* LO (147.2 cm^{-1}) phonons. In $Pb_{1-x}Eu_xTe$, the transverse optical phonon originating from the TO phonon frequency of pure EuTe can be traced down to a Eu concentration of $x=0.02$, where it appears as a local mode at 127 cm^{-1}, well above the LO frequency of PbTe. Hence, it does not evolve into the TO frequency of PbTe, as would be required in the one-mode behavior expected from the relative masses, dielectric constants, and force constants.[37] Barring an unlikely mode crossing, we also exclude an LO mode connecting the LO frequencies of the end members. This leads to the conclusion that $Pb_{1-x}Eu_xTe$ shows *two-mode behavior* with a local mode of Eu in PbTe at 127 cm^{-1}. From the investigation of superlattices with several different thicknesses of EuTe, we determine the LO-phonon dispersion curve of EuTe along $\langle 111 \rangle$ well into the Brillouin zone. In order to obtain the phonon dispersion for bulk EuTe, strain corrections are required.

ACKNOWLEDGMENTS

This research was supported by National Science Foundation Grants No. INT-9726210 and No. DMR-9800858, by Deutscher Akademischer Auslandsdienst DAAD, Bonn and by the Fonds zur Förderung der wissenschaftlichen Forschung, Vienna, Grant No. 11557.

*Present address: Advanced Photon Source, Argonne National Laboratory, Argonne, IL 60439.
†Present address: Applied Materials, Santa Clara, CA 95050.
‡Present address: MiCRUS-M15, Hudson Valley Research Park, Hopewell Junction, NY12544.

[1] F. Geist, W. Herbst, C. Mejia-Garcia, H. Pascher, R. Rupprecht, Y. Ueta, G. Springholz, G. Bauer, and M. Tacke, Phys. Rev. B **56**, 13042 (1997).
[2] H. Krenn, W. Herbst, H. Pascher, Y. Ueta, G. Springholz, and G. Bauer, Phys. Rev. B **60**, 8117 (1999).
[3] M. Tacke, B. Spanger, A. Lambrecht, P.R. Norton, and H. Böttner, Appl. Phys. Lett. **53**, 2260 (1988).

[4] D.L. Partin, IEEE J. Quantum Electron. **24**, 1716 (1988).
[5] D. L. Partin, in *Strained-Layer Superlattices: Materials Science and Technology*, Vol. 33 of *Semiconductors and Semimetals*, edited by R. K. Williardson and A. C. Beer (Academic, New York, 1991), p. 331.
[6] Z. Feit, M. McDonald, R. Woods, V. Archembault, and P. Mak, Appl. Phys. Lett. **68**, 738 (1996).
[7] P. Wachter, CRC Crit. Rev. Solid State Mater. Sci. **3**, 189 (1972).
[8] J. Schoenes, Z. Phys. B **20**, 345 (1975).
[9] J. Schoenes and P. Wachter, Physica B **86-88**, 125 (1977).
[10] L.E. Schmutz, G. Dresselhaus, and M.S. Dresselhaus, J. Magn. Magn. Mater. **11**, 412 (1979).
[11] G.D. Holah, J.S. Webb, R.B. Dennis, and C.R. Pidgeon, Solid State Commun. **13**, 209 (1973).
[12] M. Ikezawa and T. Suzuki, J. Phys. Soc. Jpn. **35**, 1556 (1973).
[13] R.B. Barnes and M. Czerny, Z. Phys. **72**, 447 (1931).
[14] D.W. Berreman, Phys. Rev. **130**, 2193 (1963).
[15] M.D. Sciacca, A.J. Mayur, Eunsoon Oh, A.K. Ramdas, S. Rodriguez, J.K. Furdyna, M.R. Melloch, C.P. Beetz, and W.S. Yoo, Phys. Rev. B **51**, 7744 (1995).
[16] R. Fuchs, K.L. Kliewer, and W.J. Pardee, Phys. Rev. **150**, 589 (1966).
[17] K.L. Kliewer and R. Fuchs, Phys. Rev. **144**, 495 (1966).
[18] K.L. Kliewer and R. Fuchs, Phys. Rev. **150**, 573 (1966).
[19] F. Proix and M. Balkanski, Phys. Status Solidi **32**, 119 (1969).
[20] B. Lou, Solid State Commun. **76**, 1395 (1990).
[21] T. Dumelow and D.R. Tilley, J. Opt. Soc. Am. A **10**, 633 (1993).
[22] Y.A. Pusep and A.I. Toropov, J. Phys.: Condens. Matter **4**, L525 (1992).
[23] B. Samson, T. Dumelow, A.A. Hamilton, T.J. Parker, S.R.P. Smith, D.R. Tilley, C.T. Foxon, D. Hilton, and K.J. Moore, Phys. Rev. B **46**, 2375 (1992).
[24] V. Sears, Neutron News **3**, 26 (1992).
[25] G. Springholz and G. Bauer, Phys. Rev. B **48**, 10 998 (1993).
[26] G. Springholz and G. Bauer, Appl. Phys. Lett. **62**, 2399 (1993).
[27] G. Springholz, N. Frank, and G. Bauer, Appl. Phys. Lett. **64**, 2970 (1994).
[28] G. Springholz, Mater. Sci. Forum **182-184**, 573 (1995).
[29] E. Koppensteiner, G. Springholz, P. Hamberger, and G. Bauer, J. Appl. Phys. **74**, 6062 (1993).
[30] BOMEM Inc., 450 St. Jean Baptiste Avenue, Quebec, Quebec G2E 5S5, Canada.
[31] Infrared Laboratories, Inc., 1808E. 17th Street, Tucson, AZ 85719.
[32] Janis Research Company, Inc., 2 Jewel Drive, Wilmington, MA 01887-0896.
[33] W. Kaiser, W.G. Spitzer, R.H. Kaiser, and L.E. Howarth, Phys. Rev. **127**, 1950 (1962).
[34] A. Krost, B. Harbecke, R. Faymonville, H. Schlegel, E.J. Fantner, K.E. Ambrosch, and G. Bauer, J. Phys. C **18**, 2119 (1985).
[35] G. Abstreiter, M. Cardona, and A. Pinczuk, in *Light Scattering in Solids IV*, Vol. 54 of *Topics in Applied Physics*, edited by M. Cardona and G. Güntherodt (Springer, Berlin, 1984), p. 5.
[36] A.S. Barker and A.J. Sievers, Rev. Mod. Phys. **47**, Suppl. No. 2 (1975).
[37] I.F. Chang and S.S. Mitra, Adv. Phys. **20**, 359 (1971).
[38] E. Jahne, Phys. Status Solidi B **75**, 221 (1976).
[39] Y. Ousaka, O. Sakai, and M. Tachiki, Solid State Commun. **23**, 589 (1977).
[40] W. Cochran, R.A. Cowley, G. Dolling, and M.M. Elcombe, Proc. R. Soc. London, Ser. A **293**, 433 (1966).
[41] A.K. Sood, J. Menéndez, M. Cardona, and K. Ploog, Phys. Rev. Lett. **54**, 2111 (1985).
[42] Eunsoon Oh, A.K. Ramdas, T. Fromherz, W. Faschinger, G. Bauer, and H. Sitter, Phys. Rev. B **48**, 17 364 (1993).